Biofouling on cementitious materials: Durability challenges across different exposure zones in marine environments

Deeksha Margapuram[1,2]

1. *LMDC, Université de Toulouse, UPS, INSA, 135 avenue de Rangueil, 31077, Toulouse Cedex 4, France*
2. *LMGC, IMT Mines Alès, University of Montpellier, CNRS, 30100 Alès, France*

RESUME

Investigating the durability aspect associated to biofouling on cementitious systems in marine environments is crucial. The presence of micro- and macro-organisms in seawater creates favourable conditions for the colonization of different cementitious systems, further complicating their performance over time. Therefore, this study investigates the influence of biofouling on plain concrete and reinforced concrete (RC) using CEM I and CEM V cement types in submerged and tidal exposure zones of a marine environment, Banyuls-sur-mer, France. Irrespective of the cement type, the microstructural analysis of submerged concrete revealed the development of biomineralized serpulid tubes on its surface. With respect to RC systems, both with and without galvanic anode cathodic protection (using aluminium anode) in the tidal zone, the half-cell potential (HCP), mixed potential, and protection current were continuously monitored upto 95 days. Furthermore, the effect of biofilm and water levels were assessed. The corrosion characteristics of embedded reinforcement in concrete were affected due to the physical barrier effect of biofilm (developed on concrete surface). This effect was observed in the average protection current of cathodic protected RC systems before and after biofilm removal. Building upon these findings creates synergy in developing ecologically durable cementitious systems that increase ecosystem functionality and strengthen infrastructure resilience.

Mots-clefs durability, biofouling, cathodic protection, marine environments, microstructure

I. INTRODUCTION

Nowadays, the expansion of marine infrastructure, particularly for renewable energy applications is largely relying on reinforced concrete (RC) as a construction material. For instance, given France's extensive coastline, offshore wind turbines (OWT) are gaining attention with projections indicating a power capacity of 18 GW by 2035 (France commits to big offshore wind volumes | WindEurope). To achieve this target, the size of the wind turbines are designed to broaden, while the service life of their support structures is expected to extend to at least 25 years (Mathern et al., 2021). However, achieving this service life may be challenging as the components (such as the support structures including floaters, seabed anchors, and so on) of OWT face several durability

challenges inherent to the marine environment. For example, floaters in the tidal exposure zone undergo repeated wetting and drying cycles, which significantly influence the durability of RC under such aggressive conditions. This often leads to initiation of corrosion of steel reinforcement in concrete. To mitigate this issue, cathodic protection (CP) for RC systems is a good solution, as investigated in this study. When CP is applied to steel in concrete, it can be implemented either using an impressed direct current system or a galvanic anode connected to the steel reinforcement. In the study, galvanic anode CP was investigated. For this type of CP, the more electronegative metals such as zinc, aluminum, and magnesium can be connected to steel reinforcement in concrete before or after initiation of corrosion (Chess, 2019). In principle, the electrochemical potential of steel in concrete shifts to protected potentials, thereby controlling corrosion. Furthermore, studies have been conducted on the influence of moisture, anode-to-cathode ratio, etc. on the performance of CP of steel reinforcement in concrete (Hassanein et al., 2002; Muehlenkamp et al., 2005; Qiao et al., 2016). But the influence of biofilm and water level on the effectiveness of galvanic anode CP is not documented, and this study addresses that gap.

Marine habitat in seawater (pH ~ 8) actively promote biofouling on immersed substrates through a natural process known as biofilm formation. This involves a series of biochemical steps, starting with adsorption of water and macromolecules, followed by colonization of bacteria, diatoms, and other microorganisms in the film/slime-like extracellular polymeric substances (EPS) (Qian et al., 2022). As immersion or exposure duration increases, complex and dynamic interactions within the micro- and macrobiota enable the development of macrofouling species, such as barnacles, mussels, polychaetes, calcareous macroalgae, and sponges, on the substrate. Previous studies have investigated biofouling on cementitious systems in marine environments (Bone et al., 2024; Hayek et al., 2020). However, research work in the submerged exposure depths and long-term duration with respect to concrete durability remains limited. Therefore, the originality of this research study lies in investigating biofouling-associated durability aspect using different binder systems for concrete-based OWT structures. The objective of this study is twofold; (i) understanding the interactions between biofouling, plain concrete systems of two cement types, and seawater, and (ii) evaluation of effectiveness of galvanic anode CP for RC systems in the presence of biofilm. This interdisciplinary approach entailing chemistry, engineering, and microbiology is not only complementary, but is essential in predicting the long-term longevity of OWT structures. In addition, given the limitations associated with investigation on full-scale engineered structures in marine environments, we have designed and adopted an experimental approach shown in Figure 1 to replicate the key components of OWT. Firstly, to address the support structures (such as floaters in floating OWT) in the tidal zone, we investigated RC systems with and without CP using galvanic aluminium anode by exposing RC in this exposure zone. Secondly, to replicate the seabed anchors and the cover concrete of submerged OWT parts, we immersed plain concrete at 27 m depth in seawater. In both the experimental setups, CEM I (portland cement) and CEM V (50 % portland cement, 25 % each of slag and fly ash) cement type-based concrete were prepared. These two cement types were selected due to their distinct chemical composition. As CEM V constitutes supplementary cementitious materials (SCMs), the study focused on investigating both biocolonization pattern and durability aspect in detail in this environment. Besides, there are very few in-situ studies investigating both aspects (Bone et al., 2022; Hayek et al., 2020). All the cementitious systems were exposed at the study site, Banyuls-sur-mer, France.

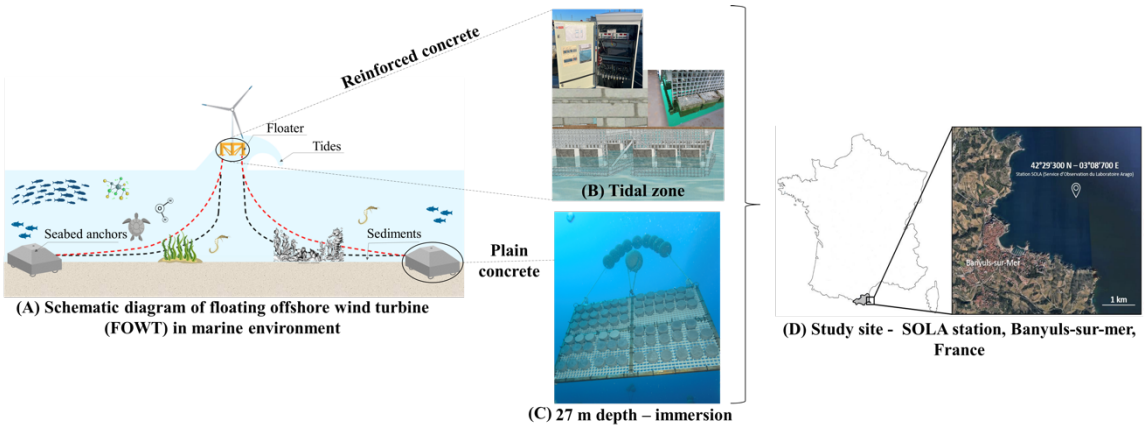

Figure 1. Two different experimental setups conducted on-site in Banyuls-sur-Mer, France (D): (B) the tidal exposure zone and (C) the submerged zone. The inset in (B) shows a photograph of grating panels with RC blocks under semi-immersed conditions.

II. INTERACTIONS BETWEEN PLAIN CONCRETE, BIOFOULING, AND SEAWATER IN THE SUBMERGED ZONE

The influence of micro- and macrofouling (known as biofouling) on plain concrete in marine environments is important to be evaluated at different exposure durations, including 1-, 3-, 18-, and 33- months. To fully understand the interactions between concrete, biofilm, and seawater, the findings presented in *Margapuram et al.* (Margapuram, 2024) reveal a detailed investigation over one- and three months exposure durations. Firstly, the microbial diversity in biofilms colonizing the concrete surfaces were analysed using environmental DNA analysis. The findings indicated that the bacterial colonization play a crucial role in biofilm formation, irrespective of cement type and exposure duration. Besides, eukaryotic colonization (or macrofouling) showed dynamic changes over time. The microbial diversity within three months exposure indicate that cement type does not play a decisive role in biofilm structuring. As a result, we infer that the short-term exposure provides a basis for long-term observations, wherein concrete is fully colonized by macrofouling organisms. At this stage, comparisons for concrete durability between two cement types is performed at microstructural scale. To facilitate this, the analytical techniques utilized in this investigation include scanning electron microscopy-energy dispersive spectroscopy (SEM-EDS), electron probe microanalysis (EPMA), and X-ray diffraction (XRD). Note that the materials, methods, and the characterizations used in this experimental work is detailed in *Margapuram et. al.* (Margapuram, 2024). Further, the following sections are divided into two, based on the type of cement, (i) CEM I and (ii) CEM V concrete.

A. CEM I concrete

Upon immersing CEM I concrete in seawater, biofilm starts forming on its surface within days to weeks. Figure 2 shows the concrete-biofilm interactions, highlighting variations in the concrete's microstructure before and after immersion, along with their corresponding Ca- and Mg-elemental maps. A comparison between the elemental maps in the control and the one-month exposure

reveals a strikingly different feature in the latter, indicating Mg precipitation (seen as a single thick layer in yellow) beneath the calcium rich deposit. This is due to the reaction between magnesium ions in seawater and the pore solution (pH ~ 13.5) of cement paste (Bonen and Cohen, 1992). Furthermore, XRD studies confirmed the presence of brucite ($Mg(OH)_2$) in Mg-layer and polymorphs of calcium carbonate, namely, calcite and aragonite in the deposit after three months exposure (Buenfeld and Newman, 1986; Margapuram, 2024). As biofouling of concrete is a time-dependent process, after three months, the surfaces are colonized with juvenile and adult biomineral-based serpulid tubes. Furthermore, at eighteen months exposure, as shown in Figure 2D, concrete surfaces were densely colonized with serpulid tubes, including other species such as macroalgae (visible to naked eye). The chemical composition of these serpulid tubes seems to be consistent for 18 months (EPMA - CaO ~ 51.9%, MgO ~ 5.8%), hinting that the chemistry of these organisms is independent of concrete so far, and mostly depend on other conditions such as Mg/Ca ions in seawater, water temperature, and other generic factors (Bornhold and Milliman, 1973).

A comparison of Mg maps at three- and eighteen- months (shown in Figure 2) reveal that the Mg layer, which was thick after three months, appears to have become thinner and discontinuous (due to dissolution) over time. This observation suggests that brucite formation is temporary and, as a result, does not effectively protect the concrete matrix from the ingress of chloride and sulphate ions. However, it may be possible that the dense calcareous serpulid tubes that colonize concrete provide long-term protection against ion diffusion, thereby modifying the kinetics over time. Furthermore, the Ca maps at three months reveal a thick deposit. These deposits seem to have dissolved over time, leaving only the calcareous serpulid tubes discernible. Overall, the colonization of calcareous serpulid species does not seem to have any detrimental effects on the concrete microstructure. Consequently, this indicates that CEM I concrete until 18 months of exposure shows no evidence of any major degradation except calcium leaching.

B. CEM V concrete

As magnesium ions are the second most abundant cations in seawater, reaction between Ca-based cement hydrates in cements with low Ca/Si (here, CEM V cement) and Mg^{2+} ions occurs. However, the formation of different Mg-hydrates such as brucite, hydrotalcite, and magnesium silicate hydrate (M-S-H) depends on the exposure duration, environmental conditions, and composition of cement (Dewitte et al., 2024). Very few studies have reported the precipitation of Mg-based hydrates in real environments, including marine and lacustrine (Jakobsen et al., 2016; Rosenqvist et al., 2017).

Following the evolution of microstructure and chemical composition over time, Figure 3A and Figure 3B shows the EPMA findings of 18-month exposed concrete and its corresponding SEM observations in BSE mode. At this exposure duration, we see significant changes in the outermost millimeters (very close to the concrete surface) of the matrix just below the calcareous serpulid tubes. The microprobe findings are shown as a function of distance from the top surface of concrete and is divided into three zones based on the chemical compositional changes. In Zones 1 and 2, we do not observe high contents of MgO (~2 %). Note that at three months exposure, MgO constituted ~ 1.5 % (Margapuram, 2024) near the surface. However, in Zone 3, the average chemical composition of CaO is 11 %, while that of MgO and SiO_2 is ~25 % each. This clearly indicates leaching of portlandite between 16-151 μm, while an enrichment of Mg-phase. This Mg-

phase could possibly be magnesium-rich silica gel, like, M-S-H (Jakobsen et al., 2016). Besides, M-S-H is favored over brucite in CEM V concrete due to its low Ca/Si ratio (inclusion of supplementary cementitious materials such as slag and fly ash), and minimum portlandite content. The reduced portlandite content leads to a drop in pH (due to decreased buffering capacity), further destabilizing C-S-H and easing the formation of M-S-H (Rosenqvist et al., 2017). Over this long duration, kinetics has changed significantly despite the colonization of calcareous serpulid tubes on the surface. This indicates that the concrete matrix has undergone slight degradation due to magnesium-rich silica gel, which possesses lower cementing properties (Jakobsen et al., 2016). This observation underscores that the chemical composition of the cement type influences the evolution of eukaryotic communities (i.e. the serpulid tubes) and may have adverse long-term effects on concrete.

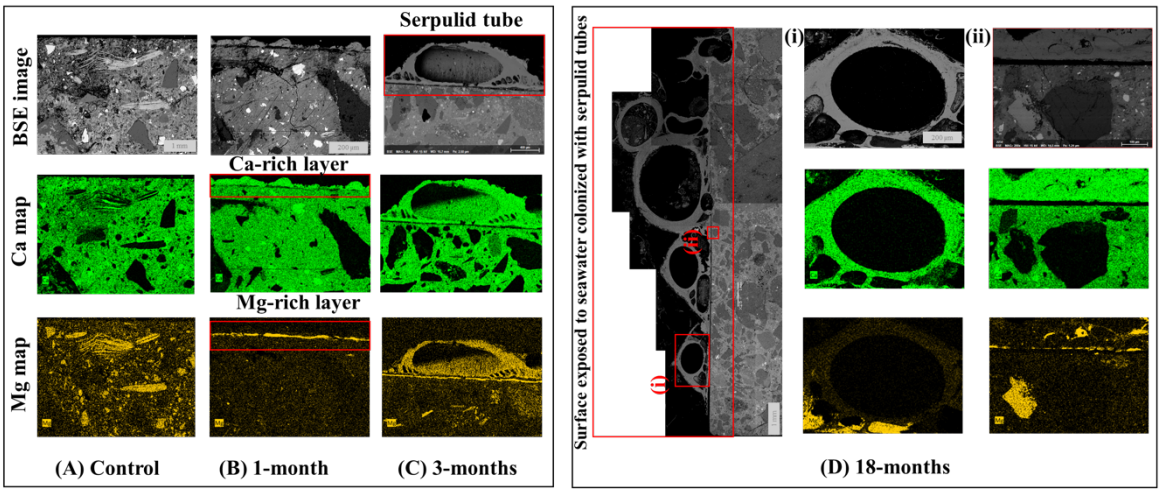

Figure 2. BSE (back scattered electron) images and corresponding Ca- and Mg- elemental maps of CEM I concrete surface submerged at 27 m depth at different exposure durations.

III. EVALUATION OF GALVANIC ANODE CP IN THE PRESENCE OF BIOFILM AND VARYING WATER LEVEL

The second objective of this study is to understand the influence of biofilm and water level on the corrosion characteristics of steel. The corrosion characteristics of steel in concrete for two cement types, both with and without cathodic protection was studied on-site (as shown in Figure 1B). Furthermore, Figure 4A shows the different components in the RC block and the assembly of steel reinforcement (diameter = 20 mm, length = 160 mm) in a grid pattern within a wooden box mold, while Figure 4B shows the photograph of a RC block having dimensions of (200 × 200 × 110) mm. To simulate marine conditions, the concrete cover was designed with a 50 mm thickness. And to ensure unidirectional ion flow into the concrete, all surfaces, except for the one exposed to biofilm formation, were coated with epoxy resin. A total of four RC blocks were prepared for the non-protected category, with two blocks for each cement type (CEM I and CEM V) and fixed to two different grating panels. For the protected category, six RC blocks were prepared, with three blocks for each cement type. All the grating panels along with the RC blocks were fixed under the harbour wharf. In addition, for galvanic CP, an external aluminium anode was placed in seawater at a depth of ~ 500 mm from the center of each grating panel (Margapuram et al., 2025).

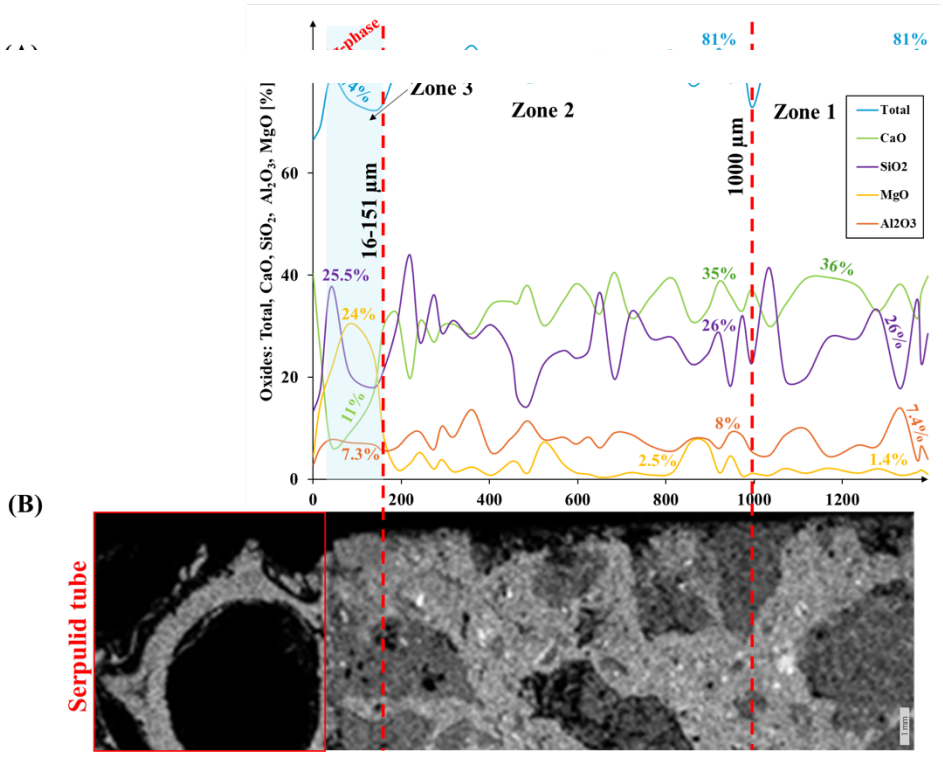

Figure 3. (A) Chemical composition profile of cement in CEM V concrete characterized using electron microprobe indicating the presence of M-S-H; and (B) Corresponding SEM observation of a polished section in BSE mode.

All the electrical connections were made to a keysight data acquisition system for recording electrochemical potential and current. The half-cell potential (HCP) was recorded for non-protected RC, while both protection current and mixed potential were recorded for galvanic CP systems continuously for every 15 minutes over 95 days. Here, protection current refers to the current supplied to steel reinforcement by the galvanic anode to mitigate corrosion by maintaining the steel at a more negative electrochemical potential. While mixed potential refers to the electrochemical potential recorded from both steel reinforcement and the galvanic anode versus the MnO_2 reference electrode. It is important to note that the electrochemical potential measured using MnO_2 reference electrode are presented on the saturated Copper/Copper Sulfate ($Cu/CuSO_4$) electrode scale to enable easier comparison with the available literature. An ultrasonic water level sensor measured the tidal heights, which were later converted to relative specimen height (in cm) to segregate the water level data and better understand its influence on corrosion characteristics under different conditions. The effectiveness of Al anode in CP for steel in concrete for two cement types is assessed with the electrochemical potential data. To note this, the initial potential of the reinforcement was monitored for 15 hours, and upon connection to Al anode across all RC blocks (CEM I: – 470 mV_{CSE} to –559 mV_{CSE} and CEM V: –230 mV_{CSE} to –330 mV_{CSE}). Polarization resulted in a shift towards a more negative potential across all RC, ranging between –580 mV_{CSE} to –780 mV_{CSE}, and indicating that the aluminum anode used in this study delivered effective CP.

To study biofilm aspects, electrochemical data with and without biofilm is required. To acquire data without biofilm, biofilm on RC blocks were removed with a sterile swab after 80 days. Electrochemical potential data, recorded 25 days before and after biofilm removal, was utilized to evaluate the corrosion characteristics of steel in concrete. Firstly, for non-protected RC blocks, **Erreur ! Source du renvoi introuvable.** (top) shows that, irrespective of cement type and water level, the HCP exhibit increased stability and less variability in the absence of biofilm. This is obvious from the wider violins and the clustering of data points around the median. Secondly, with respect to varying water levels in the presence of biofilm, for instance, at higher water levels (> 15 cm), in CEM I, the variations in HCP are ~ –500 mV_{CSE} and –600 mV_{CSE}, while in CEM V, ~ –300 mV_{CSE} and –400 mV_{CSE}. This clearly shows that corrosion characteristics of steel are influenced by varying water levels. It could be attributed to the higher water saturation, with enhanced ionic conductivity and reduced oxygen availability (Liam et al., 1992). Moreover, the absence of biofilm on surfaces may allow oxygen diffusion, resulting in corrosion activities at the steel and, thus, stable HCPs. In contrast, the presence of biofilm may generate a potential gradient in oxygen concentration within the biofilm itself, while also influencing the concrete-biofilm interface (De Beer et al., 1994). For RC blocks with galvanic CP (as shown in Figure 5 (bottom)), the protection current increases in CEM I concrete without biofilm. In contrast, the effect in CEM V concrete is less pronounced when water levels are below 15 cm. This difference may be due to the higher concrete resistivity of CEM V concrete, which is 304 Ωm, compared to 150 Ωm in CEM I concrete. And in the absence of biofilm (as shown in Figure 5 (bottom)), the protection current in CEM V concrete is uniformly distributed within a specific range, whereas this uniformity is not observed in CEM I concrete. Finally, it is noteworthy that the biofilm does not interfere with the effectiveness of CP system with galvanic anode for RC structures (Margapuram et al., 2025). While the results from this study provide valuable insights, they are more suitable for interpreting the corrosion characteristics in a qualitative manner.

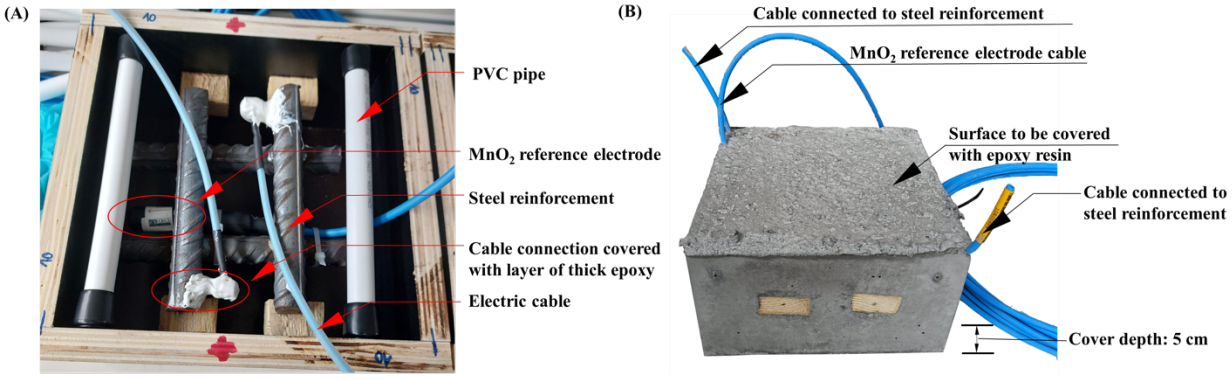

Figure 4. (A) Wooden formwork with different components in the RC block including a grid-shaped steel reinforcement and two PVC pipes on the opposite sides to suspend it on a grating panel and (B) Photograph of RC block.

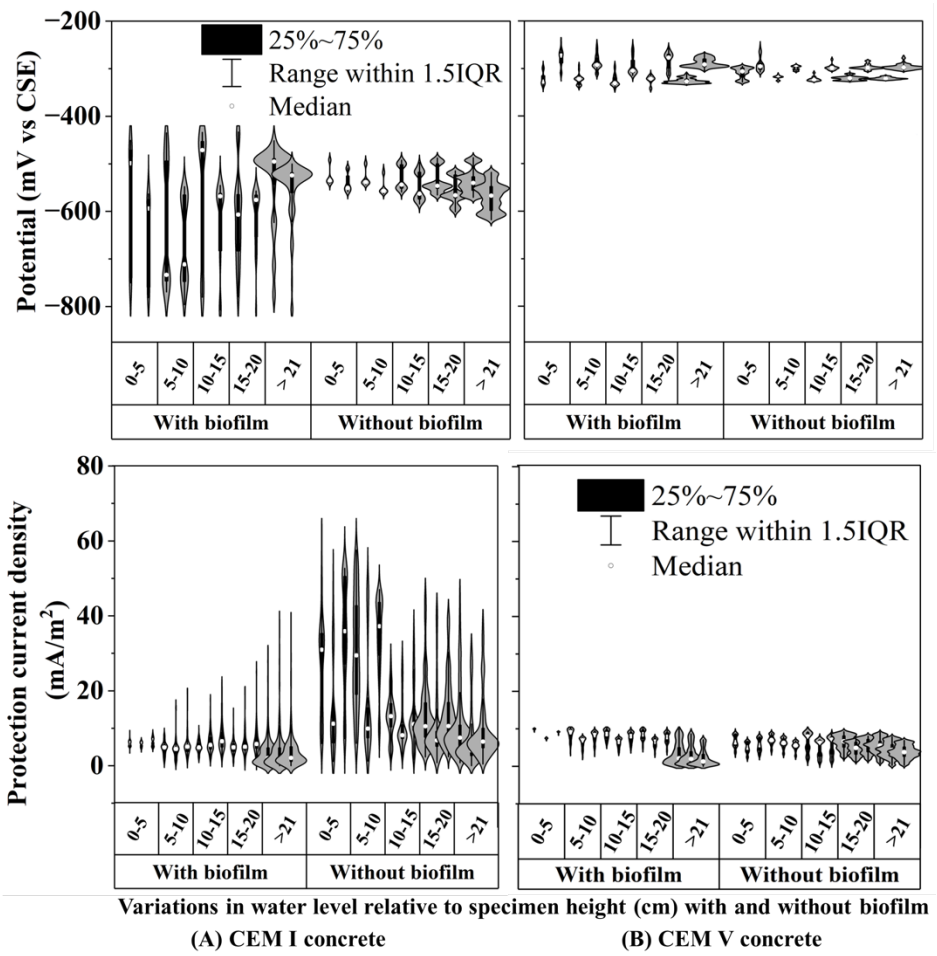

Figure 5. Violin plot distribution of HCP for the non-protected category (top) and protection current for protected category (bottom) for RC blocks, recorded for 50 days (including a 25-day dataset for conditions with and without biofilm).

IV. CONCLUSIONS

This study, with its twofold objective, has successfully addressed both; (i) the interactions between concrete, biofouling, and seawater, and (ii) the understanding of corrosion characteristics of embedded steel in concrete under the influence of biofilm and water level. This additionally offers realistic insights into the applicability of CEM I and CEM V cement types for these environments, enabling us to assess which is more appropriate for marine conditions in terms of long-term durability of structures. Firstly, the results from the 18-month exposure of the first study under submerged conditions indicate that CEM I concrete is relatively resistant to degradation, with slight calcium leaching, besides the ingress of sulphates and chlorides. Interestingly, biofouling does not appear to have any negative effects on the concrete at this stage. In contrast, CEM V exhibits distinct material behaviour, likely due to its lower Ca/Si ratio in the cement matrix. Over the long term, interactions between the concrete and seawater, combined

with the absence of calcium deposit and the reduced colonization of calcareous serpulid tubes, may contribute to the formation of magnesium hydrates, such as magnesium-rich silica gel, near the surface. These hydrates are considered to have inferior mechanical properties, making the surface more susceptible to erosion over time (Dewitte et al., 2024). CEM V has undergone slight deterioration, showing noticeable effects of biofouling. The results from the second part of this study provide novel perspectives into the corrosion characteristics of steel reinforcement in concrete, specifically comparing two binder systems with and without CP, and under the influence of biofilm and water level. The presence and absence of biofilm significantly influence the electrochemical potential of the embedded steel in concrete. This is also evident from the observed variations in protection current in protected category, where the removal of the biofilm led to an increase in the protection current, alongside, demonstrating that the Al anode performs efficiently under these conditions. Further research work should focus on investigating the microbial diversity of biofilm which is crucial in understanding the electrochemical activity of steel in concrete, and the long-term protection system efficiency in these environmental conditions. Then understanding how plain concrete systems interact with its microbial communities and assessing its role in either deterioration or protection over time is essential.

ACKNOWLEDGEMENTS

This research study is funded by Region Occitanie (*DuMaCoBio* project). The project acknowledges Wind'Occ agency for its federation and connection support during the construction and operation, and to the Bio2Mar (K. Escoubeyrou) and *Remimed* technical platforms.

REFERENCES

Bone, J.R., Hall, A.E., Stafford, R., Herbert, R.J.H., 2024. Inconsistent bioreceptivity of three mortar mixes in subtidal sites. Ecological Engineering 204, 107265. https://doi.org/10.1016/j.ecoleng.2024.107265

Bone, J.R., Stafford, R., Hall, A.E., Herbert, R.J.H., 2022. The intrinsic primary bioreceptivity of concrete in the coastal environment – A review. Developments in the Built Environment 10, 100078. https://doi.org/10.1016/j.dibe.2022.100078

Bonen, D., Cohen, M.D., 1992. Magnesium sulfate attack on portland cement paste-I. Microstructural analysis. Cement and Concrete Research 22, 169–180. https://doi.org/10.1016/0008-8846(92)90147-N

Bornhold, B.D., Milliman, J.D., 1973. Generic and Environmental Control of Carbonate Mineralogy in Serpulid (Polychaete) Tubes. The Journal of Geology 81, 363–373. https://doi.org/10.1086/627876

Buenfeld, N.R., Newman, J.B., 1986. The development and stability of surface layers on concrete exposed to sea-water. Cement and Concrete Research 16, 721–732. https://doi.org/10.1016/0008-8846(86)90046-3

Chess, P.M., 2019. Cathodic protection for reinforced concrete structures, CRC focus. CRC Press, Boca Raton London New York.

De Beer, D., Stoodley, P., Roe, F., Lewandowski, Z., 1994. Effects of biofilm structures on oxygen distribution and mass transport. Biotech & Bioengineering 43, 1131–1138. https://doi.org/10.1002/bit.260431118

Dewitte, C., Lacarrière, L., Neji, M., Bertron, A., Dauzères, A., 2024. Chemo-mechanical characterization of a low-pH model cement paste in magnesium bearing environment. Cement and Concrete Research 184, 107598. https://doi.org/10.1016/j.cemconres.2024.107598

Hassanein, A.M., Glass, G.K., Buenfeld, N.R., 2002. Protection current distribution in reinforced concrete cathodic protection systems. Cement and Concrete Composites 24, 159–167. https://doi.org/10.1016/S0958-9465(01)00036-1

Hayek, M., Salgues, M., Habouzit, F., Bayle, S., Souche, J.-C., De Weerdt, K., Pioch, S., 2020. In vitro and in situ tests to evaluate the bacterial colonization of cementitious materials in the marine environment. Cement and Concrete Composites 113, 103748. https://doi.org/10.1016/j.cemconcomp.2020.103748

Jakobsen, U.H., De Weerdt, K., Geiker, M.R., 2016. Elemental zonation in marine concrete. Cement and Concrete Research 85, 12–27. https://doi.org/10.1016/j.cemconres.2016.02.006

Liam, K.C., Roy, S.K., North Wood, D.O., 1992. Chloride ingress measurements and corrosion potential mapping study of a 24-year-old reinforced concrete jetty structure in a tropical marine environment. Magazine of Concrete Research 44, 205–215. https://doi.org/10.1680/macr.1992.44.160.205

Margapuram, D., 2024. Short-term interactions of concrete, biofilm, and seawater in the submerged zone of marine environments for sustainable floating offshore wind turbines. Construction and Building Materials. https://doi.org/10.1016/j.conbuildmat.2024.138840

Margapuram, D.-A., Salgues, M., Thibault, O., Lami, R., Erable, B., Groc, M., Vuillemin, R., Hesse, B., Souche, J.-C., Stratta, F., Bayle, M., Memet, J.-B., Zudaire, L., Deby, F., Laurens, S., Chalhoub, C., Sassine, E., Nougarolles, F., Kamde, D.K., Bertron, A., 2025. Field measurements of galvanic anode cathodic protection of reinforced concrete systems in marine environment: Influence of water level and biofilm. RILEM Tech Lett 9, 117–126. https://doi.org/10.21809/rilemtechlett.2024.205

Mathern, A., Von Der Haar, C., Marx, S., 2021. Concrete Support Structures for Offshore Wind Turbines: Current Status, Challenges, and Future Trends. Energies 14, 1995. https://doi.org/10.3390/en14071995

Muehlenkamp, E.B., Koretsky, M.D., Westall, J.C., 2005. Effect of Moisture on the Spatial Uniformity of Cathodic Protection of Steel in Reinforced Concrete. CORROSION 61, 519–533. https://doi.org/10.5006/1.3278188

Qian, P.-Y., Cheng, A., Wang, R., Zhang, R., 2022. Marine biofilms: diversity, interactions and biofouling. Nat Rev Microbiol 20, 671–684. https://doi.org/10.1038/s41579-022-00744-7

Qiao, G., Guo, B., Ou, J., Xu, F., Li, Z., 2016. Numerical optimization of an impressed current cathodic protection system for reinforced concrete structures. Construction and Building Materials 119, 260–267. https://doi.org/10.1016/j.conbuildmat.2016.05.012

Rosenqvist, M., Bertron, A., Fridh, K., Hassanzadeh, M., 2017. Concrete alteration due to 55years of exposure to river water: Chemical and mineralogical characterisation. Cement and Concrete Research 92, 110–120. https://doi.org/10.1016/j.cemconres.2016.11.012